Ionization energy of the phosphorus donor in 3C–SiC from the donor-acceptor pair emission

I. G. Ivanov,[1,a)] A. Henry,[1] Fei Yan,[2] W. J. Choyke,[2] and E. Janzén[1]
[1]*Department of Physics, Chemistry and Biology, Linköping University, 58183 Linköping, Sweden*
[2]*Department of Physics and Astronomy, University of Pittsburgh, Pittsburgh, Pennsylvania 15260, USA*

(Received 23 June 2010; accepted 7 August 2010; published online 24 September 2010)

Donor-acceptor pair luminescence of P–Al and N–Al pairs in 3C–SiC is analyzed. The structures in the spectra corresponding to recombination of pairs at intermediate distances are fitted with theoretical spectra of type I (P–Al pairs) and type II (N–Al pairs). It is shown that in the regions chosen for fitting the line positions obey the equation $\hbar\omega(R)=E_G-E_D-E_A+e^2/\varepsilon R$, where $\hbar\omega(R)$ is the energy of the photon emitted by recombination of a pair at a distance R, e is the electron charge, ε is the static dielectric constant, and E_G, E_D, and E_A are the electronic band gap and the donor and acceptor ionization energies, respectively. The fits yield the values $E_G-E_D-E_A$ for the N–Al (2094 meV) and P–Al (2100.1 meV) cases. Using the known value of the nitrogen ionization energy, 54.2 meV, phosphorus ionization energy of 48.1 meV is obtained. Identification of the sharp lines corresponding to recombination of close pairs in the P–Al spectrum is suggested. © *2010 American Institute of Physics*. [doi:10.1063/1.3487480]

I. INTRODUCTION

Nitrogen and phosphorus are being explored as standard shallow donors in several polytypes of silicon carbide. The former is always present even in undoped samples due to its abundance in the atmosphere, however, achieving high doping levels is hindered by its limited solubility. Phosphorus is considered as an alternative, however, the available studies of 3C–SiC mostly deal with N doped samples. Ionization energies of donors and acceptors can be estimated using the temperature dependence of the Hall-effect[1,2] but an accurate determination usually requires optical methods. An early study of the N donor in 3C–SiC demonstrates that the binding energies of p- and s-like states can be deduced from the observation of the so called two-electron transitions in the low-temperature photoluminescence (PL) spectra.[3] Their values for the electron effective mass and its anisotropy, as well as the N donor ionization energy, differ very little (~1%) from the same quantities determined in later work more accurately using completely different techniques, cyclotron resonance for the effective masses[4] and far-infrared absorption (FIRA) for the binding energies of the $1s(A_1)$ and $1s(E)$ states.[5] The FIRA is the most straightforward method for the determination of the electronic structure of a shallow donor by observation of allowed by symmetry transitions from the ground-state to p-like excited states at low-temperature. The data is usually processed within the effective-mass theory (EMT) (Ref. 6) and yields the donor ground-state energy $1s(A_1)$ (the ionization energy) and its valley-orbit split-off counterpart $1s(E)$. The N ionization energy determined in Ref. 5 is $E_N=54.2$ meV using the electron effective masses $m_\perp=0.247$ and $m_\parallel=0.677$ of Ref. 4. For comparison, the calculated within the EMT ionization energy of a shallow donor is 47.2 meV.[5] Data on P doped 3C–SiC is scarce[7] and does not allow conclusive determination of the P ionization energy.

Another fruitful approach to the determination of ionization energies is based on the analysis of the donor-acceptor pair (DAP) luminescence. The DAP spectrum of moderately doped with donors and acceptors samples consists of multiple sharp lines, the energies of which obey the equation[8]

$$\hbar\omega(R) = E_G - E_D - E_A + e^2/\varepsilon R + J(\mathbf{R}_D - \mathbf{R}_A), \quad (1)$$

where $\hbar\omega(R)$ is the energy of the photon emitted via recombination of an electron captured at a donor at radius vector $\mathbf{R}_D$ with a hole at acceptor at $\mathbf{R}_A$, $R=|\mathbf{R}_D-\mathbf{R}_A|$, e is the electron charge, ε is the static dielectric constant, and $J(\mathbf{R}_D-\mathbf{R}_A)$ is a correction term which depends not only on the donor-acceptor separation R, but also on the crystallographic orientation of the pair axis.[9,10] Some of the early studies of the DAP luminescence in SiC deal with highly doped (HD) samples,[11] in which case the spectrum consists of broad bands corresponding to remote-pair emission involving donors at inequivalent sites in the 4H and 6H polytypes and their phonon replicas.[12] However, sharp lines corresponding to emission of close *isolated* pairs have also been reported for the cases of N–Al pairs,[13] N–B pairs,[14] and N–Ga pairs.[15] In Ref. 13 the N–Al sharp lines were analyzed to obtain the quantity $\hbar\omega_\infty=E_G-E_D-E_A=2093.4$ meV but unfortunately at that time the accurate separation of the ionization energies of the donor and the acceptor was not possible. In most cases the analysis of the DAP spectra is restricted to identification of the shells responsible for the sharp lines in the spectrum. (A shell is defined as the set of possible sites for an acceptor lying on a sphere centered at a donor, or vice versa, and each shell is uniquely determined by the crystal structure and the site occupation of the donor and the acceptor). If the donors and the acceptors involved are present in moderate concentrations (from previous experience in SiC, of the order of

a)Electronic mail: iiv@ifm.liu.se.

$10^{16}-10^{17}$ cm^{-3}), the DAP spectra show not only sharp well separated lines for the close pairs, but also plenty of structure in the broad band corresponding to remote-pair recombination. In this case a fitting procedure can be applied to fit the pair emission at intermediate distances, i.e., at distances when $J(\mathbf{R}_D-\mathbf{R}_A)$ is negligible but the structure in the broad band is still prominent. Using Eq. (1) with J=0, one can obtain an accurate value of the quantity $\hbar\omega_\infty=E_G-E_D-E_A$. This procedure was employed in the case of 4H–SiC doped with N–Al (Ref. 16) and P–Al.[17] We use it here to model the spectra of N–Al and P–Al pairs in 3C–SiC. Since the ionization energy of the N-donor is known, $E_N=54.2$ meV, we are able to determine accurately also the P-donor ionization energy.

II. EXPERIMENTAL DETAILS

The N–Al sample used in this work is a single crystal Lely platelet with unintentional but rather high doping level similar to the one used in Ref. 13. The P–Al samples are inclusions of 3C–SiC in epitaxial layers of 4H and 6H SiC codoped during chemical-vapor deposition with P and Al. The thickness of the epilayers is approximately 30 μm. The PL spectra of different 3C inclusions found in the 4H or 6H layers have the same structure, the only difference being the line width of the sharp lines.[18] The P and Al concentrations measured by secondary-ion mass spectrometry are in the low-to-mid 10^{16} cm^{-3} range in the hexagonal polytypes and are probably similar in the 3C inclusions, judging from the sharpness of the structure observed in the broad band corresponding to remote pair recombination. The background N-doping level is very low (in the 10^{13} cm^{-3} range), hence the lines due to N-bound exciton (BE) are not visible in the PL spectra of the P–Al codoped 3C–SiC.

The PL is excited using the 325 nm line of a He–Cd laser for the N–Al doped sample, and the 351 nm line of an Ar^+-ion laser for the rest of the samples presented here. The laser penetration depths in 3C–SiC are 2.9 and 4.6 μm for the 325 and 351 nm lines, respectively,[19] thus any contribution from the substrate in the case of the 30 μm thick P–Al doped epitaxial layers can be neglected. The spectra are collected using a monochromator in combination with a charge coupled device camera, with spectral resolution better than 1 Å. All measurements are performed in a helium-bath cryostat at T=2 K. Low laser excitation is used for the DAP spectra, typically <1 mW at the sample focused to a spot of about 100 μm, in order to avoid extra lines associated with excited states of the pairs.

III. RESULTS AND DISCUSSION

The experimental spectra of N–Al and P–Al pairs are shown in Figs. 1(a) and 1(b). The curves in Figs. 1(c) and 1(d) are reference spectra of N-doped 3C–SiC with two different doping levels, HD and low-doped (LD). Apart from the lines associated with N-BE recombination denoted by N in the figure, the LD spectrum clearly shows the phonon replicas related to recombination of free excitons (denoted by FE). The subscript following N or FE is the approximate energy (in meV) of the momentum-conserving phonon; thus N_0 denotes the no-phonon line. Similar notation is used for the P-BE lines denoted by P in the bottom curve. Since the energy shift between the replicas of the FE and the corresponding replicas of the N-BE in the LD spectrum is ~9.5 meV, and N_0 is at 2379.5 meV, we obtain $E_{GX}\approx 2389$ meV for the excitonic band gap of 3C–SiC, in good agreement with the previous estimate 2390 meV.[20] The no-phonon line of the P-BE is barely seen in the P–Al spectrum, but its replicas appear strong and shifted toward higher energies by 1.9 meV from the corresponding N-BE replicas in the HD and LD spectra. Hence, the binding energies of excitons to N and P are 9.5 and 7.6 meV, respectively.

If the correction term $J(\mathbf{R}_D-\mathbf{R}_A)$ in Eq. (1) is neglected, all that is needed to synthesize a DAP spectrum are the lattice parameters and the dielectric constant at low-temperature ε. We use $\varepsilon=9.82$, as determined from the fit of the nitrogen FIRA spectra,[5] and the low-temperature lattice constant $a=4.3585$ Å.[21] Both type I and type II spectra are calculated (in the former case the donor and the acceptor substitute the same host atom species, whereas in the latter case they reside on different sublattices). A part of each theoretical spectrum corresponding to pairs with "intermediate" separations R (see below) is then used to fit the experimental spectrum, i.e., either the N–Al or the P–Al pair emission.

The fit of each spectrum is done by shifting the chosen part of the theoretical spectrum along the experimental one and using the least-squares method (LSM) to find the amplitude multiplying the theoretical curve and a few other parameters, which provide the best fit for each shift. The best fits for the N–Al and P–Al cases are also displayed in Fig. 1. One may anticipate that the background underlying the structure of the spectrum to be fitted will vary with the doping level, hence a polynomial background is added to the theoretical curve in the fitting, and the polynomial coefficients are the above-mentioned other parameters found using the LSM. Degrees of one to four have been tried for this polynomial without significant deterioration of the best fit or change in its position. The degrees used for the P–Al and N–Al DAP fits shown in Fig. 1 are three and four, respectively.

The fits yield the parameters $\hbar\omega_\infty^{N-Al}=E_G-E_N-E_{Al}=2094.0\pm0.2$ meV and $\hbar\omega_\infty^{P-Al}=E_G-E_P-E_{Al}=2100.1\pm0.2$ meV for the N–Al and P–Al pairs, respectively. The former value is very close to the value of 2093.4 meV determined in Ref. 13 from a fit of the energies of relatively *close* pairs (shell number m in the range $32\le m\le 80$), whereas in our fit the chosen part of the spectrum corresponds to $76\le m\le 252$ (26.8 Å$<$R$<$48.9 Å) for the N–Al case and to $58\le m\le 239$ (24.5 Å$<$R$<$49.7 Å) for the P–Al one. The neglect of $J(\mathbf{R}_D-\mathbf{R}_A)$ in these ranges of m is justified *a posteriori* by the quality of the fit. A quantitative parameter characterizing the quality of the fit is the ratio A/S, where A is the amplitude of the theoretical spectrum in the fit and S is the least-squares sum.[17] This parameter exhibits a sharp maximum at the shift for which the theoretical spectrum matches the experimental one, which in turn is verified by visual inspection of the fit. We note that for completeness we have tried to fit both pair spectra with theoretical spectra of type I and type II. As expected, the N–Al

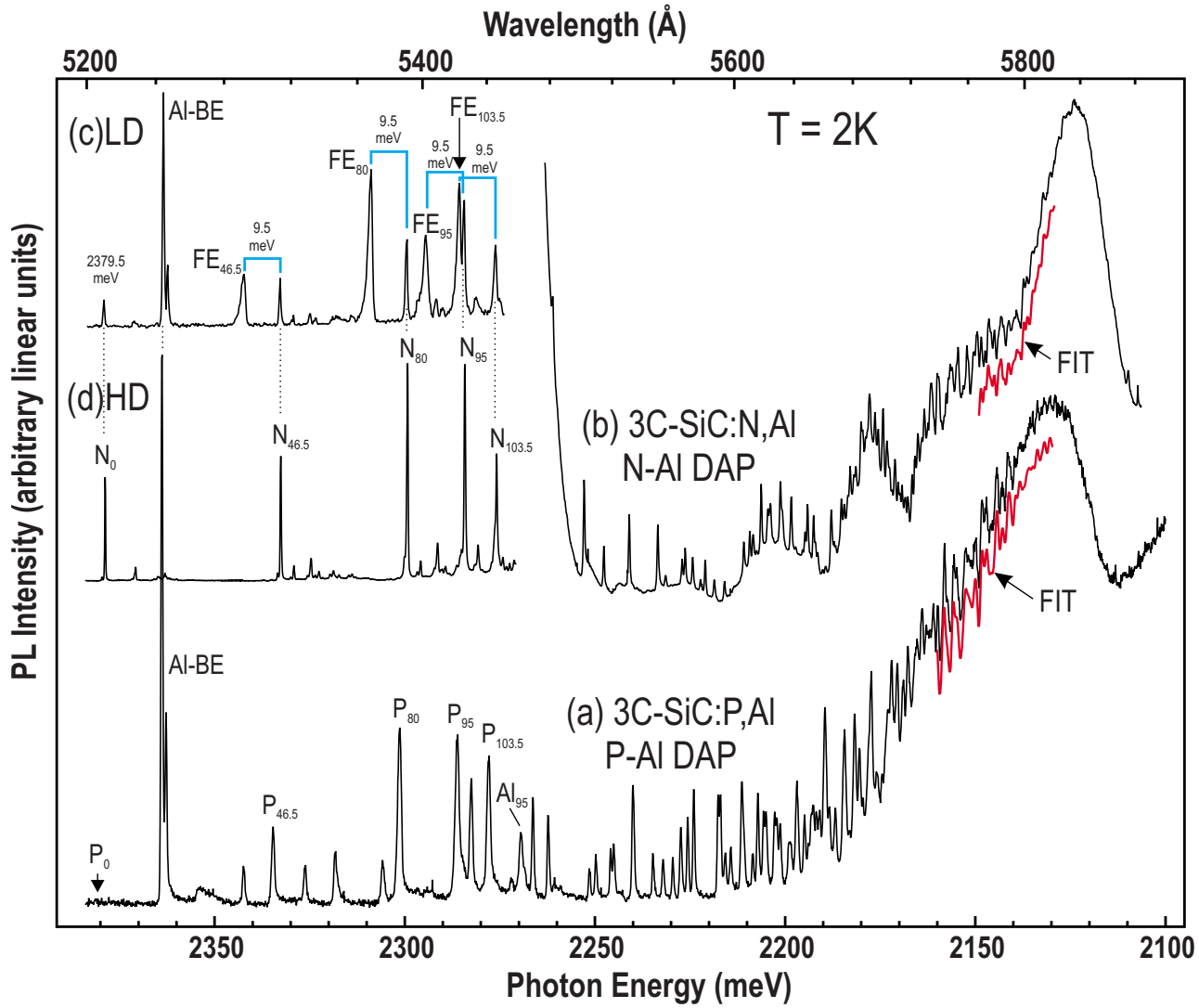

FIG. 1. (Color online) Low-temperature PL spectra showing (a) P–Al, and (b) N–Al DAP luminescence in the region of no-phonon recombination. The fits to the spectra are slightly displaced downwards for better visibility. The two spectra (c) and (d) at the top left corner are the reference spectra of the LD sample and more HD with N sample, respectively.

spectrum fits to type II, whereas the P–Al spectrum—to type I theoretical spectrum. Unlike N, which resides on carbon sites, P has been shown theoretically to be able to occupy both Si and C sites, albeit the C site has much lower probability.[22] However, we have not been able to find any contribution from P on the carbon site in our spectra.

Since the ionization energy for the N donor $E_N = 54.2$ meV is known, and the Al acceptor is the same in both cases, the ionization energy of P on Si site is easily obtained, $E_P = E_N + \hbar\omega_\infty^{N-Al} - \hbar\omega_\infty^{P-Al} = 48.1 \pm 0.4$ meV, very close to the effective-mass value (47.2 meV).[5] E_P is also within the error bar of the ionization energy of an unidentified shallow donor (47.8 meV) observed in the absorption spectra of Ref. 5, which suggest that this donor might well be due to phosphorus contamination in their sample. Assuming that the value of the FE binding energy $E_{bx} = 27 \pm 1$ meV is correct,[23] we obtain for the indirect band gap of 3C the value $E_G = 2416 \pm 1$ meV, which also agrees with the previously reported value of 2417 meV.[24] Thus, our estimate $E_{Al} = E_G - \hbar\omega_\infty^{P-Al} - E_P = 268 \pm 1$ meV of the aluminum acceptor ionization energy differs only slightly from the value 271 meV of Ref. 24. The values of the various quantities discussed are summarized in Table I.

It is interesting to carry out an identification of the sharp

TABLE I. Energies (in meV) obtained or used in this work and comparison to available literature data. The accuracy of the Al ionization energy depends on the accuracy of the binding energy of the FE E_{bx}.

	Literature data	This work
Ionization energy of P-donor on Si site, E_P	⋯	48.1 ± 0.4
Ionization energy of N-donor on C site, E_N	54.2 ± 0.2 [a]	⋯
Free-exciton binding energy, E_{bx}	27 ± 1 [b]	⋯
Excitonic band gap, E_{GX}	2390[c]	2389 ± 0.2
Electronic band gap, E_G	2417 ± 1 [d]	2416 ± 1
Al acceptor ionization energy, E_{Al}	271 ± 1 [d]	268 ± 1
Exciton binding energy to N-donor	⋯	9.5 ± 0.2
Exciton binding energy to P-donor	⋯	7.6 ± 0.2

[a]References 5 and 27.
[b]Reference 23.
[c]Reference 20.
[d]Reference 24.

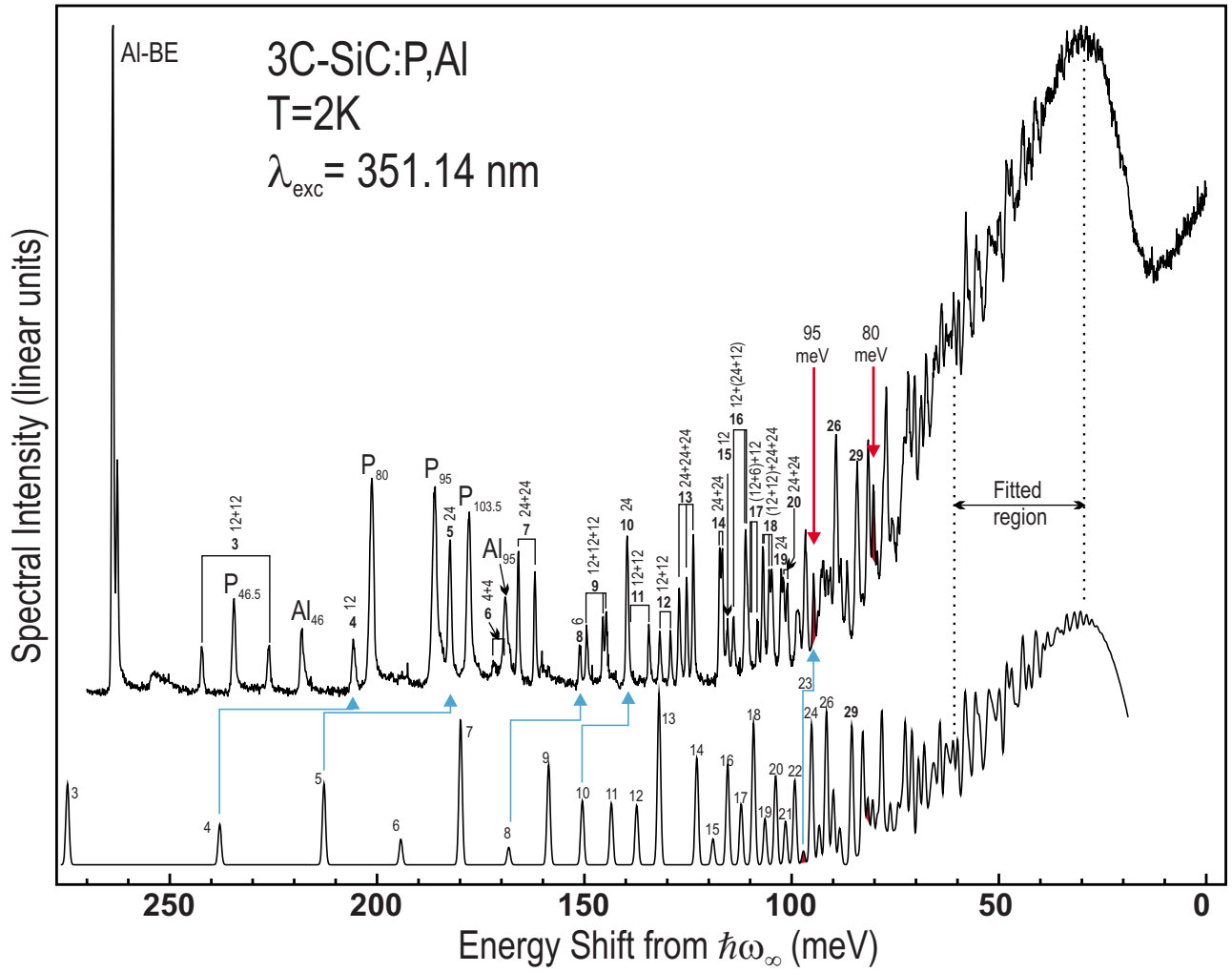

FIG. 2. (Color online) Comparison between the theoretical type I spectrum (bottom curve) and the experimental P–Al DAP spectrum illustrating the shell identification.

lines in the high-energy part of the DAP spectrum related to recombination of close pairs, using the theoretical spectrum as a base.[25] Previous analysis of the DAP luminescence in GaP, where several different species acting as donors and acceptors, have been studied earlier, shows that in some cases the splitting of the lines due to inequivalent crystallographic orientations of close pairs within the same shell can be described if the so called multipole terms are taken in account.[9,10] However, satisfactory fits have been obtained only for the C–O, Zn–O, and Cd–O pairs in GaP, which is essentially due to the small polarizability of the deep O donor ($E_D \approx 895$ meV).[13] It should be noted that the multipole corrections reflect the (nonpoint) charge distribution of the donor and acceptor cores and, therefore, provide a correction to the Coulomb energy term, i.e., to the *final* state of the pair. Corrections to the *initial* state of the pair, which is represented by the neutral donor and acceptor before recombination, have been treated in terms of van der Waals interaction using a term proportional to R^{-6} with no directional dependence. However, it is generally clear that the perturbations of the wave functions of the electron and the hole bound to closely-spaced donor and acceptor, respectively, should also exhibit pronounced directional dependence. A quantitative theory describing more accurately the interaction of the particles before recombination is not available at present. Our aim is to provide reliable identification of the shells in the line spectrum, which might serve as an experimental database for evaluation of such a theory in the future. We consider the P–Al DAP emission, and similar to previous work our identification uses the rule "equal intensities per DAP" for closely spaced lines.[13] Using the theoretical spectrum we start from the *remote* pairs and continue toward higher energies until we reach the closest pairs observed.

Figure 2 presents the results of the P–Al shell identification. Although the theoretical spectrum is calculated using Eq. (1) with $J(\mathbf{R}_D - \mathbf{R}_A) = 0$ (no account for any line splitting), it is straightforward to trace its correlation with the experimental spectrum well beyond the fitted region, down to approximately shell $m = 29$. This shell contains 96 atoms and should split into four subshells but apparently the splitting is too small to be resolved and the four components merge in a single line shifted by $E_C = e^2/\varepsilon R = 84.2$ meV from the value of $\hbar\omega_\infty^{P-Al} = 2100.1$ meV. The position of the theoretical line is 85.45 meV. Note the dip on its high-energy side which is equally well reproduced in the theoretical and

experimental spectra. When tracing the shells with $m<29$ we notice that the theoretical line positions are systematically shifted from the experimental ones toward *higher* energies and this shift increases with decreasing m as expected. Similarly, the splitting of the lines becomes resolvable for $m\leq 20$ and increases with decreasing m. It should be noted that a smooth exponential factor $\exp(-E/E_C)$ with an empirically chosen value of $E=120$ meV is applied to the theoretical curve in order to account for the decreasing overlap between the electron and hole wave functions. This choice reproduces well also the broad band corresponding to remote-pair luminescence peaking around 2130 meV.

The shells with $m\leq 20$ show resolved components, which are identified for each shell with joint vertical bars. The shell numbers m for $3\leq m\leq 20$ are labeled in bold and above each of them in a vertically oriented text we list the numbers of atoms in each subshell which stipulate approximately the relative intensities of the lines within a shell and its nearby shells. The subshells are listed in order from left to right as seen in the spectrum. The lines in the theoretical curve are also labeled with the corresponding shell numbers. Very few assumptions are made in assigning the experimental lines. Thus, we assume that some components of shells 16 and 18 are not resolved and merge into a single line. (In these cases, the two merging components are listed in brackets in the vertically oriented text, and the corresponding vertical bar is doubled.) Also, two of the components of shell 17 probably fall within the right-hand side line of shell 16, as denoted in the figure, which is supported by the larger line width of this line. The last assumption is that one of the two lines (12 atoms in each subshell) belonging to shell $m=11$ merges with the single line associated with $m=10$ (24 atoms), which explains its larger intensity. We note also that we have no clear identification of the second weak line due to shell 6, probably because it falls within the phonon replica of the Al-BE line denoted Al_{95}. The experimental shifts from $\hbar\omega_\infty^{P-Al}$ and numbers of atoms corresponding to the spectral lines associated with shells $3\leq m\leq 20$ are listed in Table II together with the calculated donor-acceptor separations R and Coulomb energies $e^2/\varepsilon R$.

It may be noted that the three components of shell 13 (24 atoms each) and shell 9 (12 atoms each) do not have exactly the same intensity, but this is not unexpected in view of the fact that for such close pairs the amount of overlap in the wave functions of the electron and the hole should depend not only on the crystallographic orientation of the pair but also on the local symmetry of each wave function, which will influence the probability of recombination and thereby the line intensity. In other words, a quantitative treatment of the splitting and the intensities of close pairs would require more elaborate model which must go beyond the $C_{\infty v}$ symmetry of the wave function envelopes in the EMT and take into account also the symmetry of the Bloch functions for the electrons and holes, as well as their mutual perturbation, which must become dominating at small separations.

A careful inspection of the line intensities in Fig. 2 suggests that we do not observe intensity anomalies in the sense discussed in Ref. 26 for GaP, where the anomalies are attributed to changes in the capturing modes. On the contrary, most of the observed intensities are consistent with the number of atoms in the corresponding subshell and the "intensity per atom" roughly smoothly decreases with increasing R.

However, certain discrete intensity anomalies can be seen. One obvious anomaly is the absence of the strong line associated with shell $m=24$. Instead, several weaker lines are observed in its place. A possible reason for this anomaly is that the values of the multipole terms V_3 and V_4 calculated by us (as defined in Ref. 9) are significantly larger for this shell than for its neighbors leading to observable splitting of this line into its four components, in contrast to its neighbors. The other two anomalies concern the increased intensity of two lines (filled and pointed out by arrows in Fig. 2) shifted from $\hbar\omega_\infty^{P-Al}$ by ~95 and ~80 meV, and corresponding to shells $m=23$ and 34. We propose that their appearance is due to peak singularities in the two-phonon density of states for the following reasons. In 3C–SiC, for most of the pairs the

TABLE II. Theoretical and experimental values of the shifts from $\hbar\omega_\infty^{P-Al}$ for the lines associated with shell numbers $3\leq m\leq 20$. The numbers of atoms and the donor-acceptor separations are also listed.

		Theoretical		
Shell no. (m)	Number of atoms	R (Å)	$e^2/\varepsilon R$ (meV)	Experimental, E_C (meV)
3a	12	5.338	274.7	242.2
3b	12			226.1
4	12	6.164	237.9	205.6
5	24	6.891	212.8	182.3
6a	4	7.549	194.2	171.7
6b	4			~169
7a	24	8.154	179.8	165.9
7b	24			161.9
8	6	8.717	168.2	151.0
9a	12	9.246	158.6	149.4
9b	12			145.5
9c	12			144.7
10	24	9.746	150.5	139.7
11a	12	10.22	143.5	~139.5
11b	12			134.4
12a	12	10.68	137.3	131.8
12b	12			129.2
13a	24	11.11	132.0	127.1
13b	24			125.3
13c	24			123.7
14a	24	11.94	122.8	117.4
14b	24			116.8
15	12	12.33	118.9	115.5
16a	12	12.71	115.4	114.0
16b	12			~111.1
16c	24			~111.1
17a	12	13.08	112.1	~110.9
17b	6			~110.9
17c	12			108.2
18a	12	13.43	109.2	106.9
18b	12			106.9
18c	24			105.4
18d	24			104.8
19	24	13.78	106.4	102.5
20a	24	14.12	103.8	101.9
20b	24			101.1

capture of either free carriers or an exciton by emission of only a single phonon is unlikely due to the large value of $E_P+E_{Al}\approx 316$ meV (in contrast to the case of C–S and Mg–S pairs in GaP, see, Ref. 26). Hence, at least two phonons are required to assist the capture process. The energies of the phonons at the Brillouin zone center are $\hbar\Omega_{TO}(0)\approx 98.7$ meV, $\hbar\Omega_{LO}(0)\approx 120.5$ meV, and at the X-point where the conduction and excitonic band minima are positioned, $\hbar\Omega_{TA}(X)\approx 46.5$ meV, $\hbar\Omega_{LA}(X)\approx 80$ meV, $\hbar\Omega_{TO}(X)\approx 95$ meV, and $\hbar\Omega_{LO}(X)\approx 103.5$ meV. The only phonon with energy less than E_P is $\hbar\Omega_{TA}(X)$ but an electron-first capture with emission of a single 46.5 meV phonon is only possible for very remote pairs where no spectral structure is observed. A capture of an exciton is always possible, but then at least two phonons $\hbar\Omega_1$ ($\mathbf{k}_1$) and $\hbar\Omega_2$ ($\mathbf{k}_2$) have to be created to conserve the energy, subject to the restriction $\mathbf{k}_1+\mathbf{k}_2=\mathbf{k}_X$, the wave vector at the X-point. The latter restriction is required by momentum conservation. Data on the two-phonon density of states subject to this restriction is not available, however, one may expect peaks at or near the combinations of one phonon from the zone center with one phonon from the X-point. A simple calculation of the eight possible combinations of this type yields that the capture of an *exciton* with simultaneous emission of $\hbar\Omega_{TO}(0)+\hbar\Omega_{TO}(X)$ would produce increased intensity of the spectrum at a shift ~95 meV, and, similarly, the combinations $\hbar\Omega_{TO}(0)+\hbar\Omega_{LO}(X)$, $\hbar\Omega_{LO}(0)+\hbar\Omega_{LA}(X)$, and $\hbar\Omega_{LO}(0)+\hbar\Omega_{TO}(X)$ correspond to shifts ~87 meV, 88.5 meV, and 73.5 meV, respectively. Consequently, the two observed discrete anomalies at $e^2/\varepsilon R\sim 95$ and 80 meV in the experimental spectrum are not in good enough agreement with such simple explanation.

Since an electron and a hole captured at a DAP can be considered as an exciton captured at the pair, it is interesting to consider some energy relations in connection with our shell identification. If an exciton is captured at the pair so that both the donor and the acceptor are in their ground states, the energy of the system is of order of $E_G-E_D-E_A$ (roughly, with all possible corrections neglected). Consequently, the energy ΔE to be given to the lattice in order to capture an exciton is of order of

$$\Delta E = E_{GX} - E_C - (E_G - E_D - E_A) = E_{GX} - E_C - \hbar\omega_\infty^{P-Al}. \quad (2)$$

At small D-A separations when the Coulomb term E_C approximated in our estimate by $e^2/\varepsilon R$ has large values, ΔE becomes negative and the capture of an exciton (or, moreover, of separate carriers) becomes impossible. Since $E_{GX}=2389$ meV, we estimate that the maximum value of the Coulomb term in a pair capable to capture an exciton is ~290 meV. Although this is just a rough estimate because we disregard all corrections to the initial and the final states of the pair in our energy balance, it agrees reasonably well with the observed *minimum* shell number $m=3$ in the spectrum (the highest-energy DAP line belonging to $m=3$ according to our identification appears shifted by ~240 meV from $\hbar\omega_\infty^{P-Al}$). According to the theoretical spectrum in Fig. 2 all shells with $m\geq 3$ ensure $e^2/\varepsilon R<290$ meV. Thus, our identification of the shells seems to be plausible.

Finally, it is useful to summarize the results of the analysis of the P–Al spectrum and the reference spectra in Fig. 1 obtained in this study. The ionization energy of phosphorus on silicon site is established to be $E_P=48.1\pm 0.4$ meV. The error margin is a consequence of the accuracy of our measurement and that of $E_N=54.2\pm 0.2$ meV.[27] The excitonic band gap is $E_{GX}=2389$ meV, and if the value of the FE binding energy $E_{bx}=27\pm 1$ meV (Ref. 23) is correct, we obtain for the indirect band gap of 3C the value $E_G=2416\pm 1$ meV, and for the aluminum acceptor ionization energy $E_{Al}=268\pm 1$ meV, in accord with previous studies.[24] No contribution from P on carbon sites could be identified in the observed spectra, which is consistent with the low probability of P residing on C sites calculated in Ref. 22.

ACKNOWLEDGMENTS

Support from the Swedish Research Council and the Knut and Alice Wallenberg Foundation is gratefully acknowledged. F.Y. and W.J.C. thank the II-VI Foundation for partial support of their research.

[1] G. Pensl and W. J. Choyke, Physica B **185**, 264 (1993).
[2] H. Matsuura, H. Nagasawa, K. Yagi, and T. Kawahara, J. Appl. Phys. **96**, 7346 (2004).
[3] P. J. Dean, W. J. Choyke, and L. Patrick, J. Lumin. **15**, 299 (1977).
[4] R. Kaplan, R. J. Wagner, H. J. Kim, and R. F. Davis, Solid State Commun. **55**, 67 (1985).
[5] W. J. Moore, P. J. Lin-Chung, J. A. Freitas, Jr., Y. M. Altaiskii, V. L. Zuev, and L. M. Ivanova, Phys. Rev. B **48**, 12289 (1993); the results of the full EMT calculation of the donor levels in 3C-SiC (without involving interpolation) are presented in E. Janzén, A. Gali, A. Henry, I. G. Ivanov, B. Magnusson, and N. T. Son, in *Defects in Microelectronic Materials and Devices*, edited by D. M. Fleetwood, S. T. Pantelides, and R. D. Schrimpf (CRC Press, Boca Raton, FL, 2009), Chap. 21, p. 621.
[6] R. A. Faulkner, Phys. Rev. **184**, 713 (1969).
[7] S. A. Padlasov and V. G. Sidyakin, Sov. Phys. Semicond. **20**, 462 (1986), to the best of our knowledge, this is so far the only reference mentioning Hall-effect measurement on intentionally P-doped 3C–SiC.
[8] D. G. Thomas, M. Gershenzon, and F. A. Trumbore, Phys. Rev. **133**, A269 (1964).
[9] L. Patrick, Phys. Rev. Lett. **21**, 1685 (1968).
[10] L. Patrick, Phys. Rev. **180**, 794 (1969).
[11] M. Ikeda, H. Matsunami, and T. Tanaka, Phys. Rev. B **22**, 2842 (1980); H. Kuwabara, S. Shiokawa, and S. Yamada, Phys. Status Solidi A **16**, K67 (1973); M. P. Lisitza, Y. S. Krasnov, V. F. Romanenko, M. B. Reifman, and O. T. Sergeev, Opt. Spectrosc. **28**, 264 (1970).
[12] In 3C–SiC there are no inequivalent sites. In 4H (one hexagonal, one cubic site) and 6H SiC (one hexagonal, two cubic sites) the donors at cubic sites are much deeper than at the hexagonal site, whereas the Al acceptor ionization energy shows very little site dependence. That is why the observation of different remote-pair bands in 4H and 6H polytypes is attributed to donors at different sites, see also Ref. 11.
[13] W. J. Choyke and L. Patrick, Phys. Rev. B **2**, 4959 (1970).
[14] H. Kuwabara, S. Yamada, and S. Tsunekawa, J. Lumin. **12–13**, 531 (1976).
[15] H. Kuwabara, K. Yamanaka, and S. Yamada, Phys. Status Solidi A **37**, K157 (1976).
[16] I. G. Ivanov, B. Magnusson, and E. Janzén, Phys. Rev. B **67**, 165211 (2003).
[17] I. G. Ivanov, A. Henry, and E. Janzén, Phys. Rev. B **71**, 241201(R) (2005).
[18] The spectrum showing the sharpest lines was used in Figs. 1 and 2.
[19] S. G. Sridhara, T. J. Eperjesi, R. P. Devaty, and W. J. Choyke, Mater. Sci. Eng., B **61–62**, 229 (1999).
[20] W. J. Choyke, Mat. Res. Bull. Vol. **4**, S141 (1969).

[21]A. Taylor and R. M. Jones, in *Silicon Carbide: A High Temperature Semiconductor*, edited by J. R. O'Connor and J. Smiltens (Pergamon, London, 1960), p. 147.
[22]M. Bockstedte, A. Mattausch, and O. Pankratov, Appl. Phys. Lett. **85**, 58 (2004).
[23]R. G. Humphreys, D. Bimberg, and W. J. Choyke, Solid State Commun. **39**, 163 (1981).
[24]W. J. Choyke, in *The Physics and Chemistry of Carbides, Nitrides, and Borides*, NATO ASI Series E Vol. 185 edited by R. Freer (Kluwer, Dordrecht, 1990), p. 563.
[25]We enumerate the shells for type I spectrum in ascending order of D-A separations using consecutive numbers $m=1,2,\ldots$, i.e., we do not omit in this sequence the "missing" shells 14, 30, etc., as is done, e.g., in Ref. 8.
[26]P. J. Dean and L. Patrick, Phys. Rev. B **2**, 1888 (1970).
[27]W. J. Moore, J. A. Freitas, Jr., and P. J. Lin-Chung, Solid State Commun. **93**, 389 (1995).